

RESEARCH

Open Access



Proteins from toad's parotoid macroglands: do they play a role in gland functioning and chemical defence?

Krzysztof Kowalski^{1*} , Paweł Marcińskiak² and Leszek Rychlik³

Abstract

Background Parotoid gland secretion of bufonid toads is a rich source of toxic molecules that are used against predators, parasites and pathogens. Bufadienolides and biogenic amines are the principal compounds responsible for toxicity of parotoid secretion. Many toxicological and pharmacological analyses of parotoid secretions have been performed, but little is known about the processes related to poison production and secretion. Therefore, our aim was to investigate protein content in parotoids of the common toad, *Bufo bufo*, to understand the processes that regulate synthesis and excretion of toxins as well as functioning of parotoid macroglands.

Results Applying a proteomic approach we identified 162 proteins in the extract from toad's parotoids that were classified into 11 categories of biological functions. One-third (34.6%) of the identified molecules, including acyl-CoA-binding protein, actin, catalase, calmodulin, and enolases, were involved in cell metabolism. We found many proteins related to cell division and cell cycle regulation (12.0%; e.g. histone and tubulin), cell structure maintenance (8.4%; e.g. thymosin beta-4, tubulin), intra- and extracellular transport (8.4%), cell aging and apoptosis (7.3%; e.g. catalase and pyruvate kinase) as well as immune (7.0%; e.g. interleukin-24 and UV excision repair protein) and stress (6.3%; including heat shock proteins, peroxiredoxin-6 and superoxide dismutase) response. We also identified two proteins, phosphomevalonate kinase and isopentenyl-diphosphate delta-isomerase 1, that are involved in synthesis of cholesterol which is a precursor for bufadienolides biosynthesis. STRING protein-protein interaction network predicted for identified proteins showed that most proteins are related to metabolic processes, particularly glycolysis, stress response and DNA repair and replication. The results of GO enrichment and KEGG analyses are also consistent with these findings.

Conclusion This finding indicates that cholesterol may be synthesized in parotoids, and not only in the liver from which is then transferred through the bloodstream to the parotoid macroglands. Presence of proteins that regulate cell cycle, cell division, aging and apoptosis may indicate a high epithelial cell turnover in parotoids. Proteins protecting skin cells from DNA damage may help to minimize the harmful effects of UV radiation. Thus, our work extends our knowledge with new and important functions of parotoids, major glands involved in the bufonid chemical defence.

Keywords Anurans, *Bufo bufo*, Bufonids, Cholesterol synthesis, IDI1, Phosphomevalonate kinase, Toad poison

*Correspondence:

Krzysztof Kowalski
k.kowalski@umk.pl

Full list of author information is available at the end of the article



© The Author(s) 2023. **Open Access** This article is licensed under a Creative Commons Attribution 4.0 International License, which permits use, sharing, adaptation, distribution and reproduction in any medium or format, as long as you give appropriate credit to the original author(s) and the source, provide a link to the Creative Commons licence, and indicate if changes were made. The images or other third party material in this article are included in the article's Creative Commons licence, unless indicated otherwise in a credit line to the material. If material is not included in the article's Creative Commons licence and your intended use is not permitted by statutory regulation or exceeds the permitted use, you will need to obtain permission directly from the copyright holder. To view a copy of this licence, visit <http://creativecommons.org/licenses/by/4.0/>. The Creative Commons Public Domain Dedication waiver (<http://creativecommons.org/publicdomain/zero/1.0/>) applies to the data made available in this article, unless otherwise stated in a credit line to the data.

Background

Amphibians inhabit a diverse range of environments worldwide [1, 2]. As amphibiotic organisms they require water reservoirs to complete their larval development. After metamorphosis most species, like bufonid toads, are usually terrestrial [1]. The migration from an aquatic to a more hybrid (semaquatic and terrestrial) environment led to many unique traits in amphibian evolution. For instance, amphibian skin plays a crucial role in their adaptation to the terrestrial environment, being responsible for respiration, water balance regulation, excretion, temperature control, osmotic changes, reproduction, and also defence [3–5]. The tegument contains two types of specialized glands, termed mucous and granular (or poison) glands. The latter form in bufonids large parotoid macroglands located in the postorbital region (Fig. 1A) [3, 4] and are involved in chemical defence [6–8].

Poison secreted from parotoids is used to protect against fungi, microorganisms and predators [9–14], as it may be irritating and even lethal for the latter [6, 13]. The chemical compounds contained in parotoid secretions have been classified into four main categories: (i) biogenic amines, such as adrenaline, noradrenaline, bradykinin, or histamine; (ii) bufadienolides; (iii) alkaloids, such as batrachotoxin or tetrodotoxin, and (iv) peptides and proteins

[4, 5, 11–13, 15]. Bufadienolides are the major components of the bufonid parotoid secretion responsible for its toxicity [8, 11, 15]. According to Steyn and Heerden [16], the toad gland secretion may contain up to 86 types of bufadienolides, including arenobufagin, bufalin, bufo- genin, bufotalin, cinobufagin, cinobufotalin, gamabufotalin, marinobufagin, and telocinobufagin [8, 11, 17].

Recently, some peptides and proteins have been identified in the toad parotoid secretions [12, 13, 18–24], but their abundance seems to be much lower than those of bufadienolides and biogenic amines [4, 12]. For instance, Sousa-Filho et al. [20] obtained 104 proteins, including actin, beta-actin, ribosomal proteins, catalase, galectin, and uncharacterised proteins, in the *Rhinella schneideri* parotoid secretion by proteomic analysis. No peptides were found. Huo et al. [25] identified 939 unique peptides by de novo approach in parotoid macrogland secretion of *Bufo gargarizans*. Mariano et al. [23] identified 42 proteins and sequenced de novo 153 peptides in the *Duttaphrynus melanostictus* skin secretion. The most common proteins were acyl-CoA-binding protein, alcohol dehydrogenase, calmodulin, catalase, galectin, proteasome subunit alpha- and beta-type, and histone. It is assumed that bufonid parotoid gland secretions do not contain bioactive peptides similar to those from the skin of many frog species [4, 12]. It has been also suggested that peptides from parotoid secretion of *Rhinella marina* could be breakdown products of larger proteins that ensure the proper gland functioning [12, 23]. However, our previous results indicate that some proteins from parotoid secretion of *Bufo bufo* may participate in the toad chemical defence [13].

Most studies of bufonid chemical defence focused on the biochemistry and pharmacology of parotoid gland secretions. Little is known about the functioning of parotoid macroglands and processes that regulate toxin biosynthesis, poison production and excretion. Therefore, to understand these processes, in this work we aimed to investigate protein content in the extract from parotoid macroglands. As a model species we used the common toad, *Bufo bufo*, which is known for producing potent poison in its parotoids [13, 26]. Some proteins and peptides, such as muscle creatine kinase, proteasome subunit α type, phospholipid hydroperoxide glutathione peroxidase, cytotoxic T-lymphocyte protein, serine/threonine-protein kinase, so far have successfully been identified in this species [13].

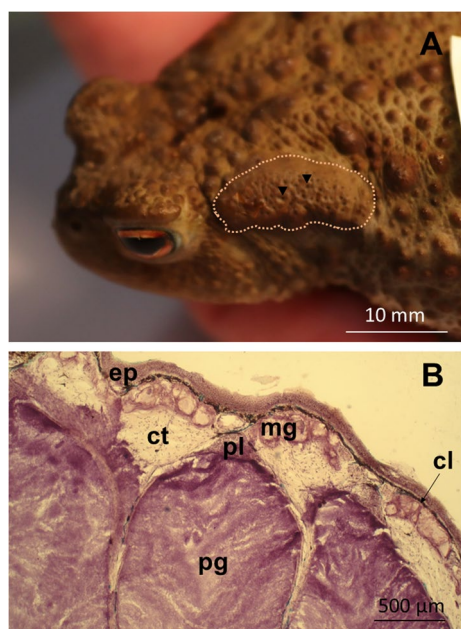


Fig. 1 **A** Female common toad *Bufo bufo* exhibiting the left parotoid macrogland (dashed line) localized at the postorbital region. Black triangles point to the glandular pores. **B** Longitudinal section of parotoid bottle-shaped glands. Abbreviations: cl—chromatophore layer; ct—connective tissue; ep—epidermis; mg—mucous glands; pg—poison glands; pl—epithelial plug. Photos by Anna Kowalczevska (**A**) and Krzysztof Kowalski (**B**).

Materials and methods

Toads trapping and housing

Trapping of toads was performed from March to April in 2016. Adult female toads *Bufo bufo* were captured

(using 10-L pitfalls and drift fences) in gardens and parks in Poznań (western Poland), placed into transporters and carried to the laboratory. Then, they were placed into large (46×30×28 cm, 39 l) aqua-terraria equipped with bedding (a mixture of peat and sand). The terraria were regularly irrigated to maintain the adequate humidity. Each terrarium contained a shelter (flowerpot) and a water tank to allow the toads to submerge in water. Food (mealworms and crickets) and water were provided ad libitum. The toads were kept in the breeding room under standard laboratory conditions (temperature: 21 °C; humidity: 65–70%; artificial photoperiod: 12L:12D).

Extraction of toad parotoid macroglands and sample preparation

Two toads were decapitated and their parotoid glands were carefully isolated (to not squeeze them and not release the poison) and transferred into 600 µl of methanol. Tissues were next homogenized and samples were centrifuged at 10,000×g and 4 °C for 30 min. The supernatants were collected, and the protein content was determined using a Direct Detect spectrometer (MERCK Millipore, Warsaw, Poland). Then, the supernatants were used for peptide analysis by reverse phase high-performance liquid chromatography (RP-HPLC). Separation was performed using a Dionex Ultimate 3000 chromatographic system comprising a dual pump programmable solvent module. Supernatants were analysed using a BioBasic-18 analytical column (5 µm, 150×4.6 mm; Thermo Scientific). The samples were eluted with a gradient of 5–60% acetonitrile (ACN)/0.1% TFA with a flow rate 0.5 ml/min for 55 min. The eluent was monitored at 214 nm and fractions were collected into 1.5-ml tubes.

Protein identification and analysis of their biological functions

Peptides and proteins from the methanolic extract of the toad parotoid glands were analysed by liquid chromatography coupled to tandem mass spectrometry (LC-MS/MS) using a Nano-Acquity LC system (Waters, Milford, Massachusetts, USA) and an OrbitrapVelos mass spectrometer (Thermo Electron Corp., San Jose, CA). Before performing the analysis, the proteins were subjected to an ion-solution digestion procedure. Proteins were: (1) reduced with 50 mM TCEP for 30 min at 60 °C, (2) alkylated with 200 mM MMTA for 30 min at room temperature and (3) digested overnight with trypsin (sequencing Grade Modified Trypsin—Promega V5111). Next, the samples were applied to an RP-18 precolumn (nanoACQUITY Symmetry® C18—Waters 186,003,514) using water containing 0.1% TFA as a mobile phase and were transferred to a nano-HPLC RP-18 column

(nanoACQUITY BEH C18—Waters 186,003,545). The samples were eluted with a gradient of 0–35% acetonitrile in the presence of 0.05% formic acid with a flow rate of 250 nl/min for 180 min. The column was directly coupled to the ion source of the spectrometer working within data dependent on the MS to MS/MS switch. To ensure a lack of cross contamination from previous samples, each analysis was preceded by a blank run.

The proteins were identified by a Mascot Search (Matrix Science, London, UK) against the SwissProt database. The search parameters were as follows: type of search: MS/MS Ion Search; enzyme specificity: trypsin; fixed methylthio modification of cysteine; variable modifications: methionine oxidation; mass values: monoisotopic; protein mass: unrestricted; peptide mass tolerance: 20 ppm; fragment mass tolerance: 0.1 D; number of missed cleavage sites allowed: 1; instrument type: HCD. Peptides with Mascot scores exceeding the threshold value of $p < 0.05$ were considered positively identified. The protein content was calculated based on the Exponentially Modified Protein Abundance Index (emPAI) [27].

The biological functions of the identified proteins were determined by searching the UniProt database. All functions were then classified into 11 categories (Table 1). The percentage of proteins displaying particular functions from each category was calculated. To understand the cellular processes in toad's parotoids, protein-protein interaction networks were built using STRING database [28]. Because molecular data on bufonid toads are scarce, predicted interactions between identified in this work proteins were analysed based on homology to the western clawed frog *Xenopus tropicalis*, a common anuran model. Then, Gene ontology (GO) enrichment analysis was performed to predict which metabolic processes the identified proteins are involved in, and what are their molecular functions (GO molecular function analysis). KEGG analysis was carried out to predict which signalling pathways the identified proteins participate in. Finally, GO component analysis was performed to predict the localisation of particular proteins within the cell.

Results and discussion

Bufo nids are worldwide distributed amphibians [1, 2] that store potent chemical weapon in their parotoid macroglands [6–8, 13]. Most of the studies dealing with toad parotoid secretions focus on biological activities of bufadienolides, biogenic amines and alkaloids [8, 11, 15]. Therefore, these molecules and their toxic and pharmacological effects are particularly well characterised [8]. Little is known about the protein and peptide content in the bufo nids, as well as their toxic properties.

Table 1 Categories of biological functions and number of proteins identified in the extract from parotoids of the common toad *Bufo bufo* displaying particular functions

Function category	Biological function	No. of proteins
1—Cell division & cell cycle regulation	Cell division, cell cycle cytokinesis, cell proliferation, cell cycle regulation/control/progression, cell growth control, mitotic cell cycle, mitosis regulation, DNA replication	34
2—Cell differentiation & tissue development	Cell differentiation, angiogenesis, skeletal muscle tissue development, epidermis development, bone development, morphogenesis	17
3—Cell migration	(Regulation of) cell migration	8
4—Cell structure maintenance	Cytoskeleton organisation, microtubules structure, actin filament organisation, intermediate filament cytoskeleton organisation, mitochondrial genome maintenance, Golgi organisation, membrane structure, regulation of cell shape, blood vessel diameter maintenance, extracellular matrix assembly, cell adhesion	24
5—Cell aging & apoptosis	Aging, apoptosis, programmed cell death (regulation)	21
6—Signal transduction	Signal transduction, cell signalling (pathway)	15
7—Metabolism	Biosynthesis, anabolism, catabolism, transcription and translation regulation, glycolysis, proteolysis, protein degradation, protein homeostasis, protein folding, protein ubiquitination, phosphorylation, intracellular pH reduction, cell motility, neurotropic and neuroprotective activity, regulation of heart rate, muscle contraction, wound healing, protein secretion, regulation of the blood coagulation cascade	99
8—Transport	Intra- and extracellular transport, nuclear transport, ion and electron transport, protein transport, toxin transport, membrane fission, channel or molecule transporter	24
9—Stress response	Stress response, response to hydrogen peroxide, oxidative stress, hypoxia tolerance, response to xenobiotic stimulus, proteolytic stress response, heat stress response, response to increased oxygen levels, cellular hypotonic response, cell redox homeostasis	18
10—Immune response	Innate and adaptive immune response, allergic/inflammatory/antimicrobial response, cell response to interleukins (IL), regulation of macroautophagy	20
11—DNA repair	DNA repair	6

Note that because many proteins display more than one function the total number of proteins do not sum up to 162

Also, the processes related to poison production and excretion remain unknown.

Here, we identified 162 proteins in the extract from parotoid macroglands of *B. bufo* (Table 2; Additional file 1: Table A1). The most abundant (with the highest emPAI) were proteins related to the cell structure maintenance and proteins with enzymatic activities involved in metabolic pathways (see Additional file 1: Table A1). For each identified protein at least one biological function was assigned by searching UniProt database (Table 2). Then, all functions were assigned to one of 11 categories (Tables 1 and 2).

STRING protein-protein interaction network predicted for proteins identified in the extract from *B. bufo* parotoids confirms the results obtained by searching the UniProt database (Additional file 2: Fig. A1). Most proteins are related to the metabolic processes with the strongest interactions between proteins involved in glycolysis, including phosphoglucomutase (pgm1), fructose-bisphosphate aldolase (aldoa), triosephosphate isomerase (tpi1), phosphoglycerate kinase 1 (pgk1) and transaldolase (talld1). Strong interactions occur also between proteins, such as transitional endoplasmic reticulum ATPase (vcp), S-phase kinase-associated protein 1 (skp1), NEDD8 (nedd8), small ubiquitin-related modifier 2 (sumo2) and

UV excision repair protein (rad23b), that participate in stress response and DNA repair and replication. This finding indicates that proteins present in the toad parotoids may effectively protect skin cells from DNA damage and thus minimize the harmful effects of UV radiation. Similarly, the results of GO enrichment and KEGG analyses are consistent with previous findings. Most predicted genes code intracellular proteins involved in metabolic processes and stress response (see Additional file 2: Figs A2–A5).

Regarding the number of identified proteins our results seem to be similar to those obtained recently by other researchers [e.g., 20, 23, 25] (see Introduction for details). One-third (34.6%) of the identified in this work proteins are involved in cell metabolism (Fig. 2 and Additional file 2: Figs A1–A4) with many of them being related to biosynthesis, regulation of transcription and translation, and gland functioning (Table 2 and Additional file 2: Figs A1–A4). This finding is consistent with the results of protein abundance analysis. Similarly, Sousa-Filho et al. [20] found numerous proteins related to cell metabolism and cell matrix in the *R. schneideri* parotoid secretion. Here, presence of two proteins, phosphomevalonate kinase (PMVK) and isopentenyl-diphosphate delta-isomerase 1 (IDI1; Table 2), is particularly noteworthy.

Table 2 Proteins identified in the extract from parotoids of the common toad *Bufo bufo* based on tandem mass spectrometry analysis

Accession code	Ion score	Mass [Da]	Matched p peptides	Protein sequence coverage [%]	Protein name	Biological function	Function category	
Q8VIF7	4539	52,958	76	6	Selenium binding protein 1	DNA replication, protein transport, response to hydrogen peroxide	1, 8, 9	
Q410Y2	2490	41,986	61	37	Actin, cytoplasmic 1	Cell motility, transcription regulation	7	
Q216W4	1425	59,993	38	13	Catalase	Aging, apoptosis regulation, cholesterol and haemoglobin metabolism	5, 7	
Q4R5L2	1262	47,371	24	14	Alpha-enolase	Glycolysis, cell growth control, hypoxia tolerance, allergic responses	1, 7, 9, 10	
P07323	630	47,433	9	8	Gamma-enolase	Neurotropic and neuroprotective activity, response to xenobiotic stimulus	7, 9	
P13929	624	47,233	8	8	Beta-enolase	Glycolysis	7	
P0C273	1019	14,949	23	31	Ubiquitin 60S ribosomal protein L40	DNA repair, cell cycle regulation, protein degradation, cell signalling	1, 6, 7, 11	
A2Q0Z1	985	71,038	23	17	Heat shock cognate 71 kDa protein	Proteolytic stress response, cell cycle regulation	1, 9	
P06761	85	72,440	3	3	78 kDa glucose regulated protein	Stress response, toxin transport, regulation of cell migration and apoptosis, cell response to IL-4	3, 5, 8–10	
P62258	906	29,293	13	11	14–3–3 protein epsilon	Cell response to heat, mitotic cell cycle regulation	1, 9	
Q5RAD2	841	16,827	21	41	Calmodulin	Calcium signal transduction pathway, cell cycle regulation, regulation of heart rate, cytokinesis regulation	1, 6, 7	
Q2QD07	815	26,912	18	18	Triosephosphate isomerase	Glycolysis	7	
A2Q0Z0	695	50,369	15	11	Elongation factor 1-alpha 1	Protein biosynthesis	7	
Q5R7H8	658	5050	19	43	Thymosin beta-4	Cytoskeleton organisation, cell cycle regulation, cell migration, regulation of inflammatory response	1, 3, 4, 10	
Q63610	599	29,173	15	18	Tropomyosin alpha-3 chain	Regulation of muscle contraction, cytoskeleton organisation	4, 7	
Q5NW0	454	58,395	10	7	Pyruvate kinase PKM	Glycolysis, regulation of cytoplasmic translation, regulation of programmed cell death	5, 7	
Q3ZBT1	450	89,826	21	12		Stress response, apoptosis, DNA repair	5, 9, 11	
Q3MHMS	431	50,167	10	10		Transitional endoplasmic reticulum ATPase		
Q32L4I	379	44,831	5	11		Tubulin beta-4B chain	Microtubules structure, mitotic cell cycle	1, 4
						Phosphoglycerate kinase 1	Glycolysis, cell response to hypoxia, epithelial cell differentiation	2, 7, 9

Table 2 (continued)

Accession code	Ion score	Mass [Da]	Matched peptides	Protein sequence coverage [%]	Protein name	Biological function	Function category
Q32L4I	336	9597	6	11	GTP cyclohydrolase I feedback regulatory protein	Phosphorylation	7
Q2PFW2	321	10,910	4	12	Small ubiquitin-related modifier 2	Nuclear transport, DNA replication, mitosis regulation, signal transduction	1,6,8
A5A6I5	312	39,777	4	3	Fructose-bisphosphate aldolase A	Glycolysis, regulation of cell migration	3,7
Q1RMJ6	297	22,268	3	8	Rho-related GTP-binding protein Rhoc	Signal transduction, cell migration, actin filament organisation, cell cycle cytokinesis	1,3,4,6
Q8N6N7	293	9830	16	11	Acyl-CoA-binding domain-containing protein 7	Fatty acid metabolism	7
Q2PFL9	273	25,087	7	8	Peroxiredoxin-6	Cell protection against oxidative stress	9
Q5R5H2	258	68,554	5	4	V-type proton ATPase catalytic subunit A	Intracellular pH reduction, protein transmembrane transport, response to increased oxygen levels	7–9
Q60218	252	36,181	6	2	Aldo-keto reductase family 1 member B10	Cellular detoxification of aldehyde	7
Q3SYU9	245	99,093	6	2	Major vault protein	Signal transduction, nucleo-cytoplasmic transport	6,8
P28768	231	15,675	3	9	Superoxide dismutase [Mn], mitochondrial	Aging, apoptosis, cell response to oxidative stress	5,9
P41361	223	52,728	5	3	Antithrombin-III	Regulation of the blood coagulation cascade	7
Q5R495	209	58,272	3	2	Serine/threonine protein kinase OSR1	Phosphorylation, cellular hypotonic response, intracellular signal transduction	6,7,9
Q4FZU2	209	59,489	4	1	Keratin, type II cytoskeletal 6A	Cell differentiation, wound healing, antimicrobial humoral immune response	2,7,10
Q3TXS7	208	106,490	3	1	26S proteasome non-ATPase regulatory subunit 1	Protein homeostasis, regulation of protein catabolism	7
Q4FZY0	208	26,743	3	5	EF-hand domain-containing protein D2	B-cell apoptosis control	5
Q4KMA2	208	43,516	3	7	UV excision repair protein RAD23 homolog B	DNA repair, cell response to IL-7	10,11
P30838	206	50,685	6	5	Aldehyde dehydrogenase, dimeric NADP-preferring	Lipid metabolism, xenobiotic metabolism	7
Q9CR51	204	13,808	4	9	V-type proton ATPase subunit G 1	Cell response to increased oxygen levels	9
P19483	198	59,775	3	5	ATP synthase subunit alpha, mitochondrial	Aging, apoptosis, lipid metabolism, electron transport	5,7,8

Table 2 (continued)

Accession code	Ion score	Mass [Da]	Matched p peptides	Protein sequence coverage [%]	Protein name	Biological function	Function category
P48644 Q8HZM6	191 177	55,276 38,943	4 3	3 3	Retinal dehydrogenase 1 Annexin A1	Oxidoreductase activity Innate and adaptive immune response, actin cytoskeleton organisation	8 4,10
P51857	175	37,629	9	9	3-oxo-5-beta-steroid 4-dehydrogenase	Bile acid biosynthesis	7
A6NEC2	174	54,127	4	4	Putumycin-sensitive aminopeptidase-like protein	Proteolysis	7
Q2HJ86	174	50,802	3	7	Tubulin alpha-1D chain	Cell division, cell response to IL-4, microtubule cytoskeleton organisation	1,4,10
Q3ZC84	173	52,990	3	3	Cytosolic non-specific dipeptidase	Proteolysis	7
COHJG9 P10111	170 156	22,571 18,047	3 6	4 9	Annexin A2 Peptidyl-prolyl cis-trans isomerase A	Angiogenesis, heat stress response Apoptosis	2,9 5
P29117	44	22,072	2	8	Peptidyl-prolyl cis-trans isomerase F, mitochondrial	Apoptosis	5
Q3MH4	153	48,021	4	6	Adenosylhomocysteinase	Chronic inflammatory response, response to hypoxia	9,10
Q4R5L1	148	46,548	2	3	Aspartate aminotransferase, cytoplasmic	Biosynthesis of α -glutamate	7
Q4PLJ0 Q46650	144 139	90,66 41,207	5 3	17 3	NEDD8 Alcohol dehydrogenase class-2 isozyme 2	Cell cycle control, proteolysis Ethanol oxidation	1,7 7
Q3TOM7	137	23,836	7	9	Ran-specific GTPase-activating protein	Nucleo-cytoplasmatic transport	8
Q5E987	136	26,532	2	7	Proteasome subunit alpha type-5	Proteasomal protein catabolism	7
Q9IKB3 Q5E946 Q2HWU2 Q3THS6	135 133 126 120	38,790 20,161 57,590 43,937	1 4 4 4	4 7 1 11	Y-box binding protein 3 Protein deglycase DJ-1 Protein disulfide-isomerase S -adenosylmethionine synthase isoform type-2	Apoptosis DNA repair Cell response to IL-7 S -adenosylmethionine biosynthesis	5 11 10 7
A3FKF7	116	35,981	3	4	Glyceraldehyde-3-phosphate dehydrogenase	Immune and antimicrobial response	10
Q3T0X5	112	29,797	3	6	Proteasome subunit alpha type-1	Proteolysis, immune response	7,10

Table 2 (continued)

Accession code	Ion score	Mass [Da]	Matched p peptides	Protein sequence coverage [%]	Protein name	Biological function	Function category
O35945	111	54,921	1	2	Aldehyde dehydrogenase, cytosolic 1	Ethanol metabolism	7
P00168	111	10,026	6	49	Cytochrome b5 (Fragment)	Electron transport	8
Q76KP1	108	116,855	7	1	N-acetyl-beta-glucosaminyl-glycoprotein 4-beta-N-acetylgalactosaminidyltransferase	Transferase activity	7
P61458	106	12,024	4	29	Pterin-4-alpha-carbinolamine dehydratase	Tetrahydrobiopterin biosynthesis	7
Q5R844	99	17,057	3	8	Myosin light polypeptide 6	Muscle contraction, skeletal muscle tissue development	2,7
Q15276	96	99,551	2	1	Rab GTPase-binding effector protein 1	Apoptosis, protein transport	5,8
Q5RF7	94	70,782	2	2	Polyadenylate-binding protein 1	mRNA processing, cell response to hypoxia	7,9
P21836	89	68,447	4	1	Acetylcholinesterase	Neuronal apoptosis, cell adhesion	4,5
Q9UBC2	85	94,289	2	1	Epidermal growth factor receptor substrate 15-like 1	Endosomal transport	8
P35908	83	65,623	1	1	Keratin, type II cytoskeletal 2 epidermal	Epidermis development	2
Q8HXW4	82	97,457	2	1	Glycogen phosphorylase, muscle form	Glucagon metabolism	7
Q52178	73	55,569	2	4	Nicotinamide phosphoribosyltransferase	Signal transduction	6
Q9DAW9	72	36,544	2	6	Calponin-3	Regulation and metabolism of smooth muscle contraction	7
Q8V73	71	37,500	2	4	Transaldolase	Carbohydrate metabolism	7
Q3ZD7	71	30,790	2	2	Carboxyl reductase [NADPH] 1	Epithelial cell differentiation	2
AOA1F3	68	36,892	1	3	L-lactate dehydrogenase A chain	Glycolysis	7
Q6IA69	68	80,291	4	1	Glutamine-dependent NAD(+) synthetase	NAD biosynthesis	7
O95340	68	69,916	1	2	Bifunctional 3'-phosphoadenosine 5'-phosphosulfate synthase 2	Blood coagulation, bone development, hormone metabolism, phosphorylation	2,7

Table 2 (continued)

Accession code	Ion score	Mass [Da]	Matched p peptides	Protein sequence coverage [%]	Protein name	Biological function	Function category
Q5RBES5	65	36,001	2	3	GDP-L-fucose synthase	Leukocyte cell–cell adhesion	4
Q4R4R7	64	35,069	1	4	Ribose-phosphate pyrophosphokinase 2	Nucleotide biosynthesis, phosphorylation	7
Q9Y2G7	63	63,081	8	3	Zinc finger protein 30 homolog	Transcription regulation	7
Q9CWM4	59	14,246	2	17	Prefoldin subunit 1	Protein folding and stabilisation	7
Q8ZP9	58	72,826	5	1	GAS2-like protein 1	Cytoskeleton structure	4
Q96CQ1	57	34,536	4	2	Solute carrier family 25	Mitochondrial genome maintenance	4
Q8IUE6	57	13,987	3	5	Histone H2A type 2B	Regulation of replication and transcription, DNA repair	1,7,11
Q4R4X6	57	23,669	1	5	Ras-related protein Rab-2A	Golgi organisation, intracellular protein transport	4,8
Q2TBX6	55	26,413	1	3	Proteasome subunit beta type-1	Proteolysis	7
Q5XHY7	54	57,491	1	1	Signal transducing adapter molecule 2	Signal transduction, membrane fission	6
A6QLU8	54	48,623	5	1	Nucleoredoxin	Cell differentiation	2
Q9D1G2	54	22,132	2	4	Phosphomevalonate kinase	Cholesterol biosynthesis	7
Q0P5K3	53	17,173	1	7	Ubiquitin-conjugating enzyme E2	Protein ubiquitination	7
Q5BJP9	52	32,716	2	4	Phytanoyl-CoA dioxygenase domain-containing protein 1	Oxidoreductase activity	8
Q4R5E4	52	61,678	1	2	Phosphoglucomutase-1	Glycolysis	7
Q00560	51	32,562	2	3	Syntenin-1	Actin cytoskeleton organisation, regulation of cell growth, migration and proliferation	1,3,4
Q5NVA2	49	55,315	1	1	Thioredoxin reductase 1, cytoplasmic	Cell population proliferation, signal transduction	1,6
Q3ZCF3	49	18,784	1	7	S-phase kinase-associated protein 1	Cell cycle progression, signal transduction, transcription regulation, protein ubiquitination	1,6,7
Q08782	48	36,547	2	2	Aldose reductase-related protein 2	Polyl metabolism, retinal metabolism	7
Q3U821	48	95,127	2	1	WD repeat-containing protein 75	rRNA processing	7
Q00915	47	15,974	1	6	Retinol-binding protein 1	Retinol transport in blood plasma	8

Table 2 (continued)

Accession code	Ion score	Mass [Da]	Matched p peptides	Protein sequence coverage [%]	Protein name	Biological function	Function category
D3KU66	46	41,175	3	2	Acetylserotonin O-methyltransferase	Lipid metabolism, melatonin biosynthesis	7
Q8BK48	46	62,599	2	1	Pyrethroid hydrolase Ces2e	Prostaglandin metabolism	7
Q9CPU0	46	20,934	2	3	Lactoylglutathione lyase	Carbohydrate metabolism, regulation of transcription and apoptosis	5,7
P02747	45	25,941	3	3	Complement C1q subcomponents subunit C	Immune response	10
A6QQV6	45	79,661	2	1	Protein arginine N-methyltransferase 7	Cell differentiation, regulation of protein binding	2,7
Q8R3H9	44	44,679	2	1	Tetratricopeptide repeat protein 4	Innate immune response, protein folding	7,10
Q68DL7	43	77,871	4	1	Uncharacterized protein C18orf63	Ubiquitin protein ligase activity	7
Q4R5E9	43	70,874	1	1	Secretogranin-2	Protein secretion, intracellular signal transduction, angiogenesis, endothelial cell migration, inflammatory response	2,3,6,7,10
A4Z6H0	43	50,343	2	3	Adenylosuccinate synthetase isozyme 1	AMP biosynthesis	7
Q5R8Y6	42	76,640	3	1	Transmembrane 9 superfamily member 2	Channel or small molecule transporter	8
Q6P6V1	41	69,685	3	1	Polypeptide N-acetylgalactosaminyltransferase 11	Signalling pathway	6
Q6ZQ82	41	92,610	2	1	Rho GTPase-activating protein 26	Actin cytoskeleton organisation, signal transduction	4,6
Q8B238	40	35,078	1	4	Serine dehydratase-like	L-serine catabolism, lipid metabolism	7
Q2MHN2	40	21,389	1	5	Ferritin heavy chain	Iron transport, immune response, regulation of cell population proliferation	1,8,10
Q96QS6	39	43,137	1	2	Serine/threonine-protein kinase H2	Protein phosphorylation	7
Q6W3E5	39	72,363	1	1	Glycerophosphodiester phosphodiesterase domain-containing protein 4	Lipid metabolism	7
Q9BXB4	37	84,188	3	1	Oxysterol-binding protein-related protein 11	Lipid transport, fat cell differentiation	2,8
Q7TQD2	37	23,698	1	5	Tubulin polymerization-promoting protein	Cell division, microtubule formation	1
Q4R362	37	11,360	1	9	Histone H4	DNA replication	1

Table 2 (continued)

Accession code	Ion score	Mass [Da]	Matched p peptides	Protein sequence coverage [%]	Protein name	Biological function	Function category
Q88879	37	142,798	2	1	Apoptotic protease-activating factor 1	Cell aging, apoptosis, cell differentiation	2, 5
Q8NEM1	37	63,275	1	1	Zinc finger protein 680	Transcription regulation	7
P97324	37	59,502	3	1	Glucose-6-phosphate 1-dehydrogenase 2	Oxidative stress, glucose metabolism, lipid metabolism	7, 9
QQVGK2	37	59,722	4	2	Tetratricopeptide repeat protein 39C	Allium assembly, otolith morphogenesis	2
Q13410	37	59,383	3	2	Butyrophilin subfamily 1 member A1	Membrane structure	4
Q2EN76	36	17,257	1	11	Nucleoside diphosphate kinase B	Cell adhesion, GTP biosynthesis, transcription, apoptosis	4, 5, 7
Q9WVW0	36	21,848	5	4	RNA-binding protein with multiple splicing	Transcription, response to oxidative stress	7, 9
P48065	35	70,380	1	1	Sodium- and chloride-dependent betaine transporter	Amino acid transport	8
Q2M2U5	35	19,844	1	3	IQ domain-containing protein F2	Calmodulin binding activity	7
Q9BE72	35	67,948	1	2	Solute carrier family 2, facilitated glucose transporter member 12	Carbohydrate metabolism, glucose import	7
Q3SWX5	35	88,484	1	1	Cadherin-6	Cell–cell adhesion	4
Q8BHF7	34	62,818	6	1	CDP-diacylglycerol-glycerol-3-phosphate 3-phosphatidyltransferase, mitochondrial	Cardiolipin biosynthesis	7
Q4V8G5	34	41,325	2	2	Septin-12	Cell differentiation, protein localization	2, 7
Q4R4W5	34	26,669	1	3	Isopentenyl-diphosphate Delta-isomerase 1	Cholesterol biosynthesis	7
Q4FZT9	34	100,768	1	1	26S proteasome non-ATPase regulatory subunit 2	Cell cycle progression, apoptosis, DNA repair	1, 5, 11
Q9NOX1	34	74,699	2	1	PR domain zinc finger protein 5	Mitotic cell cycle, transcription regulation	1, 7
B7ZNG4	33	72,650	2	1	Tastin	Cell adhesion	4
Q9EP69	33	67,361	3	1	Phosphatidylinositide phosphatase SAC1	Phosphatidylinositol biosynthesis	7

Table 2 (continued)

Accession code	Ion score	Mass [Da]	Matched peptides	Protein sequence coverage [%]	Protein name	Biological function	Function category
Q8WUM4	32	96,469	1	1	Programmed cell death 6-interacting protein	Apoptosis, protein transport	5, 8
Q35WUJ0	32	39,331	1	1	RISC-loading complex subunit TARBP2	Translation regulation, cell proliferation	1, 7
Q8TD55	32	53,593	2	1	Pleckstrin homology domain-containing family O member 2	Regulation of cell shape	4
A3KN27	32	60,420	2	2	Keratin, type II cytoskeletal 74	Intermediate filament cytoskeleton organisation	4
P48506	32	73,363	2	1	Glutamate-cysteine ligase catalytic subunit	Aging, cell redox homeostasis, blood vessel diameter maintenance	5, 7, 9
B2RZ78	32	20,594	1	5	Vacuolar protein sorting-associated protein 29	Intracellular protein transport	8
Q3TI40	31	10,983	1	16	Dynein light chain roadblock-type 1	Microtubule-based movement	4
Q8K1R7	31	108,501	4	1	Serine/threonine protein kinase Nek9	Cell cycle, cell division, protein phosphorylation	1, 7
Q5NMP9	31	37,259	3	3	Mortality factor 4-like protein 1	Cell cycle, apoptosis, transcription regulation	1, 5, 7
Q9JL24	30	21,174	1	5	Interleukin-24	Apoptosis, cell response to IL-4 and LPS, regulation of cell migration	3, 5, 10
O35774	30	94,030	2	2	A-kinase anchor protein 4	Signal transduction, establishment of protein localisation	6, 7
Q9H7P6	30	35,919	1	3	Multivesicular body subunit 12B	Membrane fission, protein transport	8
Q8CG76	30	40,954	1	2	Aflatoxin B1 aldehyde reductase member 2	Lipid metabolism	7
A2VCK2	30	37,963	2	2	Doublecortin domain-containing protein 2B	Allium assembly, neuron migration	3
A4FUB0	30	73,548	1	1	Uncharacterized protein C5orf34 homolog	Regulation of calcium ion binding	8
Q9CXW2	30	41,258	2	3	28S ribosomal protein S22, mitochondrial	Mitochondrial translation	7
Q6FRU5	29	25,248	1	3	Clathrin light chain B	Intracellular protein transport	8
Q8NGL2	29	35,272	1	2	Olfactory receptor 5L1	G protein-coupled receptor signalling pathway	6
Q4KLM6	29	80,472	1	1	Prolyl 3-hydroxylase 2	Collagen metabolism, regulation of cell population proliferation	1, 7

Table 2 (continued)

Accession code	Ion score	Mass [Da]	Matched p peptides	Protein sequence coverage [%]	Protein name	Biological function	Function category
Q9WUH5	29	56,607	2	2	Tripartite motif-containing protein 10	Erythrocyte differentiation, innate immune response	2, 10
O60336	29	165,188	1	1	Mitogen-activated protein kinase-binding protein 1	Regulation of antimicrobial response, regulation of IL-8 production, protein ubiquitination	7, 10
Q6IUU3	29	83,004	3	1	Sulphydryl oxidase 1	Extracellular matrix assembly, protein folding, regulation of macroautophagy	4, 7, 10
Q28960	29	31,949	1	2	Carboxyl reductase [NADPH] 1	Epithelial cell differentiation, glucocorticoid metabolism, xenobiotic metabolism	2, 7
Q9BZB8	29	63,245	1	2	Cytoplasmic polyadenylation element-binding protein 1	Cell response to hypoxia	9
Q9P9L6	28	160,895	2	1	Kinesin-like protein KIF15	Mitotic cell cycle, microtubule-based movement	1, 4
Q53GT1	28	72,449	1	2	Kelch-like protein 22	Cell division, cell growth regulation	1
Q5RER6	26	38,650	1	3	Serine/threonine-protein kinase PDIKL	Apoptosis, cell cycle, cell proliferation and differentiation, transcription regulation	1, 2, 5, 7

Function category: 1—Cell division & cell cycle regulation; 2—Cell differentiation & tissue development; 3—Cell migration; 4—Cell structure maintenance; 5—Cell aging & apoptosis; 6—Signal transduction; 7—Metabolism; 8—Transport; 9—Stress response; 10—Immune response; 11—DNA repair

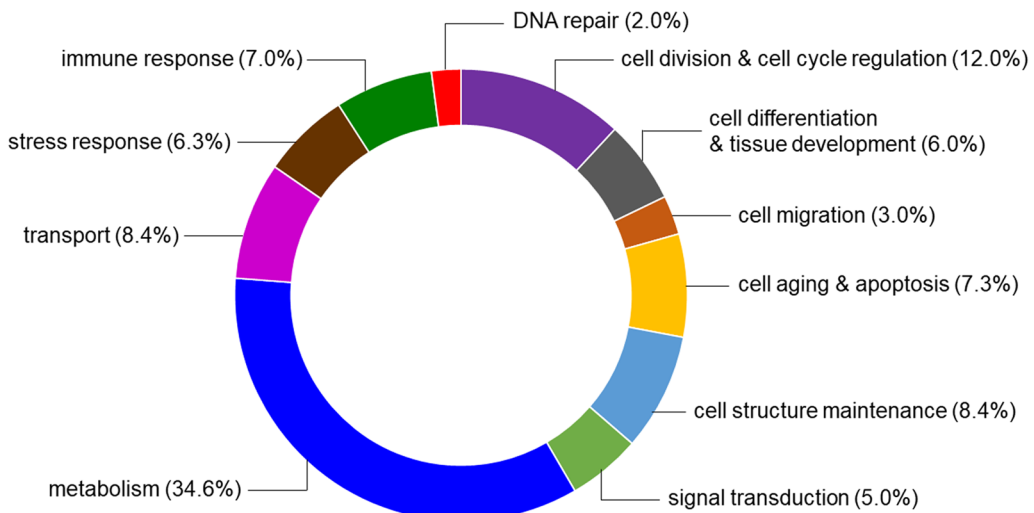


Fig. 2 Biological functions of proteins identified in the extract from parotoids of the common toad *Bufo bufo*. Values in parentheses show percentage of proteins classified into each function category. See Table 2 for detailed functions of particular proteins

These molecules are involved in the mevalonate arm of the cholesterol biosynthesis pathway [29, 30]. PMVK catalyses formation of mevalonate 5-diphosphate from mevalonate 5-phosphate, an essential step in the mevalonate pathway, while IDI1 performs isomerisation of isopentenyl diphosphate into dimethylallyl diphosphate (Fig. 3) [29, 30]. Cholesterol has been confirmed to be a precursor for synthesis of various steroids including bufadienolides [31–33], and it has been assumed that it is synthesised in the liver and then secreted and transferred through the bloodstream to the parotoid glands [31, 32]. Recent studies showed that genes coding PMVK and IDI1 are expressed in 27 human tissues including liver, kidney, spleen, adrenal glands and brain [34]. Genes coding IDI1 have been also proven to express in the liver of *X. tropicalis* frog [35]. PMVK has not been reported in any amphibian organs and tissues so far. Thus, confirming the presence of PMVK and IDI1 in the toad parotoid extract indicates that cholesterol necessary for toxin production may be also synthesised in parotoids, major glands that store bufadienolides.

Parotoids are holocrine glands [6, 36–38] in which poison excretion is accompanied by changes in the gland structure (Fig. 1B) [7]. Therefore, the complete poison replenishment is considered to be metabolically costly and time-consuming for toads [7], and may affect their growth and behaviour [39]. According to Jared et al. [7], the Cururu toad *Rhinella icterica* requires more than 3 months to restore the poison secreted from parotoids after mechanical compression of glands and the parotoid content seems to not return to the state preceding poison extraction. Rapid poison replenishment is necessary to

ensure chemical protection against predators and micro-organisms. Therefore, for toads, a reduced or depleted poison supply can be life-threatening because of diminished defence capabilities. In this work, we found various proteins involved in cell division and cell cycle regulation (12.0%), as well as cell aging and apoptosis (7.3%; Fig. 2). Together with many proteins that participate in molecule biosynthesis and transport (8.4%) as well as maintenance of cell structure (8.4%; Fig. 2), it may be indicative of a high epithelial cell turnover in parotoids. Such an intense cell turnover in the holocrine gland should require well developed protein machinery that regulates cell cycle and cell divisions to enable quick and effective replenishment of toxins and thus increase the chance of survival during encounter with a predator.

Some proteins found in this study are likely to reinforce toxic activity of parotoid secretion. For instance, gamma-enolase has neurotropic properties [40, 41] and thus its presence in parotoid secretion may increase paralytic activity of toad poison. Antithrombin-III regulates the blood coagulation cascade (Table 2) and may block blood clot formation [42, 43] and thus cause bleeding. Few proteins, such as puromycin-sensitive aminopeptidase-like protein, cytosolic non-specific dipeptidase or proteasome subunit alpha type-1, cause proteolysis [44–47] and thus may reinforce proteolytic action of toad poison. Previously, we also described in *B. bufo* parotoid secretion some peptides that may display physiological effects [13]. Mariano et al. [23] found proteasomes in *D. melanostictus* skin secretions. It is therefore likely that some molecules obtained in this work also participate in the toad chemical defence. However, further studies are required

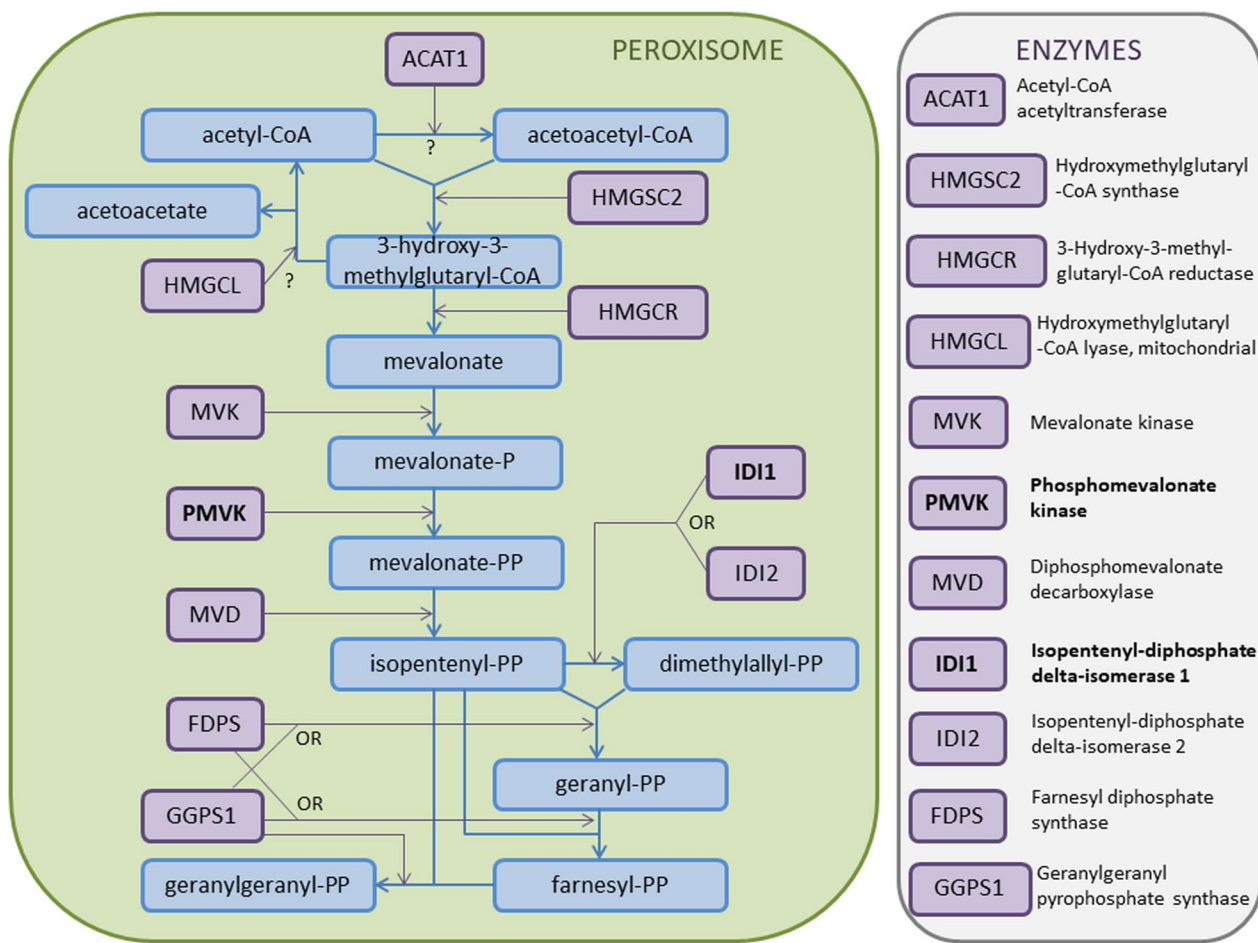


Fig. 3 The mevalonate pathway in the cholesterol biosynthesis (according to Mazein et al. [27], modified). Blue arrows indicate synthesis processes, while purple arrows catalysis accelerated by enzymes. Question marks indicate uncertain processes. Enzymes (PMVK and IDI1) identified in this work in the extract from *B. bufo* parotoids are shown in bold

to confirm their biological activity and describe their action modes.

Tropomyosin alpha-3 chain, myosin light polypeptide 6 and calponin-3 are involved in regulation of muscle contraction (Table 2) [48–50]. Calmodulin is a Ca^{+2} -binding protein that regulates apoptosis, inflammation and smooth muscle contraction [51–53]. Therefore, these proteins may promote poison excretion from parotoids. Also, 78 kDa glucose regulated protein, which is related to toxin transport [54], may participate in poison secretion from toad parotoids. Myosin light polypeptide 6 and calmodulin have already been reported in the *D. melanostictus* parotoid secretion [22, 23]. Calmodulin has been also found in the toad urinary bladder, oviduct and retina photoreceptors [55–57], while myosin and tropomyosin in smooth muscles within the carotid labyrinth of *Rh. marina* [58] and skeletal muscles of *X. tropicalis* and the Japanese tree frog *Hyla japonica* [59].

Mariano et al. [23] identified 62 binding proteins in the skin secretions of *D. melanostictus*. These proteins might bind to different molecules and play important role in amphibian skin secretion. In this work, we found acyl-CoA-binding domain-containing protein 7 and annexins in the *B. bufo* parotoid extract. The latter have been suggested to regulate diverse cellular and physiological processes, such as endo- and exocytosis [60, 61], and thus promote toxin excretion from poison glands. Both, acyl-CoA-binding proteins (ACBPs) and annexins, have recently been reported in *D. melanostictus* skin secretions [22, 23]. ACBPs have also been found in the frog's brain [62], while annexins in the skin of the large-webbed bell toad *Bombina maxima*, the Dybrowsky's frog *Rana dybowskii*, and the Chinese giant salamander *Andrias davidianus* [63–65]. It seems that the latter are unique to the skin and because of their antimicrobial activity related to the immune response of amphibian skin secretions.

It is well known that amphibian skin plays an important role in antimicrobial defence [66, 67]. Proteins related to immune defence have already been reported in anuran skin secretions [18, 66–68]. Also, in this work we found proteins involved in innate and adaptive immune response, and antimicrobial, allergic and inflammatory response (7.0%; Table 2, Fig. 2). Thus, our results confirm antimicrobial functions of bufonid skin secretions. Also, proteins related to stress response are quite abundant (6.3%) in the extract from *B. bufo* parotoids (Fig. 2 and Additional file 2: Figs A1–A3). Here, we identified catalase, peroxiredoxin 6 and superoxide dismutase that are related to the anti-oxidant system [69]. Similar proteins (catalase, glutathione peroxidase 3, peroxiredoxin 6, superoxide dismutase and thioredoxin like 1) have previously been reported in parotoid secretion of *R. schneideri* [20]. Superoxide dismutase has also been identified in skin secretions of *R. dybowskii* [64], while catalase in lungs, heart, liver and kidney of the painted frog *Discoglossus pictus* [70].

Amphibian populations are in decline, which has been exacerbated in the last few decades and caused by several factors [71]. Ultraviolet (UV) radiation is especially dangerous to amphibians because of their thin and poorly cornified integument [72], and may lead to protein denaturation, cell damage and death, and/or mutagenesis in amphibian skin [73, 74]. Amphibians can cope with the harmful effects of UV radiation in many ways which include behavioural and molecular mechanisms. Here, we report 6 proteins in the extract from toad parotoids (Table 2, Fig. 2 and Additional file 2: Fig. A1) that are involved in DNA repair. Also, heat shock proteins (HSPs) may be synthesised under environmental or physiological stress [75]. They interact with denatured proteins and help them to refold and reassemble, turning back their active forms [23, 76]. Therefore, all these molecules may represent molecular mechanisms that may effectively protect toad skin cells from DNA damage and thus minimize the harmful effects of UV radiation. Such proteins involved in protection against UV radiation damage and protein recycling have been recently found in the skin secretion of *D. melanostictus* [23]. Related to stress response HSPs have been reported for many anuran organs, such as skin, liver, heart, kidneys, lungs and brain [77, 78].

Conclusions

We report here housekeeping proteins in the extract from *B. bufo* parotoid macroglands. Applying a proteomic approach enabled us to obtain new findings on the molecules that are involved in poison production

and secretion, and may contribute to the gland functioning. Most identified proteins are involved in metabolic processes and cell structure maintenance. Our results indicate that in toads cholesterol may be synthesized in parotoids, and not only in the liver from which is then transferred through the bloodstream to the parotoids. Presence of proteins that protect skin cells from DNA damage may help to minimize the harmful effects of UV radiation. It opens up new perspectives for studying biological activity of molecules from parotoid secretions and their role in the toad chemical defence system. Applying de novo peptide sequencing coupled with analyses of various databases will provide new protein dataset in anuran skin secretions and extend our knowledge on the functioning of bufonid parotoids.

Supplementary Information

The online version contains supplementary material available at <https://doi.org/10.1186/s12983-023-00499-8>.

Additional file 1. Table A1. Peptide sequences identified in the extract from parotoids of the common toad *Bufo bufo* based on tandem mass spectrometry analysis

Additional file 2. Figures A1-A5. **Fig. A1** STRING protein-protein interaction network predicted for proteins identified in the extract from parotoids of the common toad *Bufo bufo* based on homology to *Xenopus tropicalis*. Red balls represent proteins involved in metabolic processes, while lines show interactions between proteins. The thicker the line, the stronger the interaction. Abbreviations within the balls represent protein labels. Full protein names and their labels are provided in Table A1 in Additional file 1.

Fig. A2 Number of proteins involved in metabolic processes predicted based on the Gene ontology enrichment analysis of proteins identified in the extract from parotoids of the common toad *Bufo bufo*. **Fig. A3** Molecular functions and number of proteins predicted based on the Gene ontology enrichment analysis of proteins identified in the extract from parotoids of the common toad *Bufo bufo*. **Fig. A4** Number of proteins involved in signalling pathways predicted based on the KEGG analysis of proteins identified in the extract from parotoids of the common toad *Bufo bufo*. **Fig. A5** Localisation of proteins identified in the extract from parotoids of the common toad *Bufo bufo* within the cell based on the Gene ontology component analysis

Acknowledgements

Not applicable.

Author contributions

All authors conceived and designed the experiments. KK obtained permits and captured experimental animals. KK and PM performed the experiments and analyzed the data. KK drafted the manuscript. All authors edited the draft and prepared the manuscript for publication. All authors read and approved the final manuscript.

Funding

The research was supported by the budgets of the Department of Systematic Zoology and Department of Animal Physiology and Developmental Biology (Faculty of Biology, Adam Mickiewicz University, Poznań).

Availability of data and materials

All data are available in the main text and the supplementary information files. Further information and requests for data should be directed to and will be fulfilled by the corresponding author.

Declarations

Ethics approval and consent to participate

Trapping procedure, handling, housing of animals and all analyses were performed in accordance with licenses of the Regional Director for Environmental Protection in Poznań (decision # WPNIIL.6401.142.2013.AG), the General Director for Environmental Protection (decision # DOP-oz.6401.00.6.2013.JRO), and the Directive 2010/63/EU on the protection of animals used for scientific purposes. The study was carried out in compliance with the ARRIVE guidelines.

Consent for publication

Not applicable.

Competing interest

The authors declare that they have no competing interests.

Author details

¹Department of Vertebrate Zoology and Ecology, Faculty of Biological and Veterinary Sciences, Institute of Biology, Nicolaus Copernicus University, Lwowska 1, 87-100 Toruń, Poland. ²Department of Animal Physiology and Developmental Biology, Faculty of Biology, Institute of Experimental Biology, Adam Mickiewicz University, Uniwersytetu Poznańskiego 6, 61-614 Poznań, Poland.

³Department of Systematic Zoology, Faculty of Biology, Institute of Environmental Biology, Adam Mickiewicz University, Uniwersytetu Poznańskiego 6, 61-614 Poznań, Poland.

Received: 2 March 2023 Accepted: 7 June 2023

Published online: 16 June 2023

References

- McDiarmid RW. Amphibian diversity and natural history: an overview. In: Heyer WR, Donnelly MA, McDiarmid RW, Hayek LAC, Foster MS, editors. Measuring and monitoring biological diversity: standard methods for amphibians. Washington: Smithsonian Institution Press; 1994. p. 5–15.
- Duellman WE. Patterns of distribution of amphibians: a global perspective. Baltimore: Johns Hopkins University Press; 1999.
- Toledo RC, Jared C, Brunner JA. Morphology of the large granular alveoli of the parotoid glands in toad (*Bufo ictericus*) before and after compression. *Toxicon*. 1992;30:745–53. [https://doi.org/10.1016/0041-0101\(92\)9008-S](https://doi.org/10.1016/0041-0101(92)9008-S).
- Clarke BT. The natural history of amphibian skin secretions, their normal functioning and potential medical applications. *Biol Rev Camb Philos Soc*. 1997;1997(72):365–79. <https://doi.org/10.1017/s0006323197005045>.
- Zhao Y, Jin Y, Lee WH, Zhang Y. Purification of a lysozyme from skin secretions of *Bufo andrewsi*. *Comp Biochem Physiol C*. 2006;142:46–52. <https://doi.org/10.1016/j.cbpc.2005.10.001>.
- Toledo RC, Jared C. Cutaneous granular glands and amphibian venoms. *Comp Biochem Physiol A*. 1995;111:1–29. [https://doi.org/10.1016/0300-9629\(95\)98515-I](https://doi.org/10.1016/0300-9629(95)98515-I).
- Jared SGS, Jared C, Egami MI, Mailho-Fontana PL, Rodrigues MT, Antoniazzi MM. Functional assessment of toad parotoid macroglands: a study based on poison replacement after mechanical compression. *Toxicon*. 2014;87:92–103. <https://doi.org/10.1016/j.toxicon.2014.05.020>.
- Zhan X, Wu H, Wu H, Wang R, Luo C, Gao B, Chen Z, Li Q. Metabolites from *Bufo gargarizans* (Cantor, 1842): A review of traditional use, pharmacological activity, toxicity and quality control. *J Ethnopharmacol*. 2020;246:112178. <https://doi.org/10.1016/j.jep.2019.112178>.
- Toledo RC, Jared C. Cutaneous adaptations to water balance in amphibians. *Comp Biochem Physiol A*. 1993;105:593–608. [https://doi.org/10.1016/0300-9629\(93\)90259-7](https://doi.org/10.1016/0300-9629(93)90259-7).
- Tempone AG, Carvalho Pimenta D, Lebrun I, Sartorelli P, Taniwaki NN, de Andrade Jr HF, Antoniazzi MM, Jared C. Antileishmanial and antitrypanosomal activity of bufadienolides isolated from the toad *Rhinella jimi* parotoid macrogland secretion. *Toxicon*. 2008;52:13–21. <https://doi.org/10.1016/j.toxicon.2008.05.008>.
- Abdel-Rahman MA, Hamid Ahmed S, Nabil ZI. *In vitro* cardiotoxicity and mechanism of action of the Egyptian green toad *Bufo viridis* skin secretions. *Toxicol Vitro*. 2010;24:480–5. <https://doi.org/10.1016/j.tiv.2009.09.021>.
- Rash LD, Morales RAV, Vink S, Alewood PF. *De novo* sequencing of peptides from the parotoid secretion of the cane toad, *Bufo marinus* (*Rhinella marina*). *Toxicon*. 2011;57:208–16. <https://doi.org/10.1016/j.toxicon.2010.11.012>.
- Kowalski K, Marciniak P, Rosiński G, Rychlik L. Toxic activity and protein identification from the parotoid secretion of the common toad *Bufo bufo*. *Comp Biochem Physiol C*. 2018;205:43–52. <https://doi.org/10.1016/j.cbpc.2018.01.004>.
- Kowalski K, Sawościanik O, Rychlik L. Do bufonids employ different anti-predator behaviors than ranids? Comparison among three European anurans. *Copeia*. 2018;106:120–9. <https://doi.org/10.1643/CE-16-567>.
- Gao H, Zehl M, Leitner A, Wu X, Wang Z, Kopp B. Comparison of toad venoms from different *Bufo* species by HPLC and LC-DAD-MS/MS. *J Ethnopharmacol*. 2010;131:368–76. <https://doi.org/10.1016/j.jep.2010.07.017>.
- Steyn PS, Heerden FR. Bufadienolides of plant and animal origin. *Nat Prod Rep*. 1998;15:397–413. <https://doi.org/10.1039/A815397Y>.
- Ma H, Zhou J, Jiang J, Duan J, Xu H, Tang Y, Lv G, Zhang J, Zhan Z, Ding A. The novel antidote Bezoar Bovis prevents the cardiotoxicity of toad (*Bufo bufo gargarizans* Canto) venom in mice. *Exp Toxicol Pathol*. 2012;64:417–23. <https://doi.org/10.1016/j.etp.2010.10.007>.
- Zhao Y, Jin Y, Wang JH, Wang RR, Yang LM, Lee WH, Zheng YT, Zhang Y. A novel heme-containing protein with anti-HIV-1 activity from skin secretions of *Bufo andrewsi*. *Toxicon*. 2005;46:619–24. <https://doi.org/10.1016/j.toxicon.2005.06.022>.
- Zhao Y, Jin Y, Wei SS, Lee WH, Zhang Y. Purification and characterization of an irreversible serine protease inhibitor from skin secretions of *Bufo andrewsi*. *Toxicon*. 2005;46:635–40. <https://doi.org/10.1016/j.toxicon.2005.07.003>.
- Sousa-Filho LM, Freitas CDT, Lobo MDP, Monteiro-Moreira ACO, Silva RO, Santana LAB, Ribeiro RA, Souza MHLP, Ferreira GP, Pereira ACT, Barbosa ALR, Lima MSCS, Oliveira JS. Biochemical profile, biological activities, and toxic effects of proteins in the *Rhinella schneideri* parotoid gland secretion. *J Exp Zool A Ecol Genet Physiol*. 2016;325(8):511–23. <https://doi.org/10.1002/jez.2035>.
- Mariano DOC, Messias MDG, Prezotto-Neto JP, Spencer PJ, Pimenta DC. Biochemical analyses of proteins from *Duttaphrynus melanostictus* (*Bufo melanostictus*) skin secretion: soluble protein retrieval from a viscous matrix by ion-exchange batch sample preparation. *Protein J*. 2018;37(4):380–9. <https://doi.org/10.1007/s10930-018-9780-z>.
- Mariano DOC, Messias MDG, Spencer PJ, Pimenta DC. Protein identification from the parotoid macrogland secretion of *Duttaphrynus melanostictus*. *J Venom Anim Toxins Incl Trop Dis*. 2019;25:e 20190029. <https://doi.org/10.1590/1678-9199-JVATID-2019-0029>.
- Mariano DOC, Prezotto-Neto JP, Spencer PJ, Sciani JM, Pimenta DC. Proteomic analysis of soluble proteins retrieved from *Duttaphrynus melanostictus* skin secretion by iEx-batch sample preparation. *J Proteomics*. 2019;209:103525. <https://doi.org/10.1016/j.jprot.2019.103525>.
- Alexandre LS, Braga FMS, de Oliveira PK, Coelho TLS, Fonseca MG, de Sousa RWR, Ditz D, de Castro e Sousa JM, Ferreira PMP, Dantas C, Barbosa HS, Chaves MH, Lopes Júnior CA, Vieira Júnior GM. Proteins from *Rhinella jimi* parotoid gland secretion: a comprehensive analytical approach. *Toxicon*. 2021;192:32–9. <https://doi.org/10.1016/j.toxicon.2021.01.005>.
- Huo Y, Xv R, Ma H, Zhou J, Xi X, Wu Q, Duan J, Zhou M, Chen T. Identification of <10KD peptides in the water extraction of Venenum Bufonis from *Bufo gargarizans* using nano LC-MS/MS and *de novo* sequencing. *J Pharm Biomed Anal*. 2018;157:156–64. <https://doi.org/10.1016/j.jpba.2018.05.027>.
- Kowalski K, Marciniak P, Rychlik L. Individual variation in cardiotoxicity of parotoid secretion of the common toad, *Bufo bufo*, depends on body size—first results. *Zoology*. 2020;142:125822. <https://doi.org/10.1016/j.zool.2020.125822>.
- Ishihama Y, Oda Y, Tabata T, Sato T, Nagasu T, Rappaport J, Mann M. Exponentially modified protein abundance index (emPAI) for estimation of absolute protein amount in proteomics by the number of sequenced peptides per protein. *Mol Cell Proteom*. 2005;4:1265–72. <https://doi.org/10.1074/mcp.M500061-MCP200>.

28. Szklarczyk D, Gable AL, Lyon D, Junge A, Wyder S, Huerta-Cepas J, Simonovic M, Doncheva NT, Morris JH, Bork P, Jensen LJ, von Mering C. STRING v11: protein-protein association networks with increased coverage, supporting functional discovery in genome-wide experimental datasets. *Nucleic Acids Res.* 2019;47:607–13. <https://doi.org/10.1093/nar/gky1131>.
29. Mazein A, Watterson S, Hsieh WY, Griffiths WJ, Ghazal P. A comprehensive machine-readable view of the mammalian cholesterol biosynthesis pathway. *Biochem Pharmacol.* 2013;86:56–66. <https://doi.org/10.1016/j.bcp.2013.03.021>.
30. Cerqueira NMFS, Oliveira EF, Gesto DS, Santos-Martins D, Moreira C, Moorthy HN, Ramos MJ, Fernandes PA. Cholesterol biosynthesis: a mechanistic overview. *Biochemistry.* 2016;55:5483–506. <https://doi.org/10.1021/acs.biochem.6b00342>.
31. Siperstein MD, Murray AW, Titus E. Biosynthesis of cardiotonic sterols from cholesterol in the toad, *Bufo marinus*. *Arch Biochem Biophys.* 1957;67:154–60. [https://doi.org/10.1016/0003-9861\(57\)90254-0](https://doi.org/10.1016/0003-9861(57)90254-0).
32. Porto AM, Gros EG. Biosynthesis of the bufadienolide marinobufagin in toads *Bufo paracnemis* from cholesterol-20⁻¹⁴C. *Experientia.* 1971;27:506.
33. Garraffo HM, Gros EG. Biosynthesis of bufadienolides in toads, VI: experiments with [1,2-³H]cholesterol, [21-¹⁴C]coprostanol, and 5 beta-[21-¹⁴C] pregnanolone in the toad *Bufo arenarum*. *Steroids.* 1986;48:251–7. [https://doi.org/10.1016/0039-128X\(86\)90008-5](https://doi.org/10.1016/0039-128X(86)90008-5).
34. Fagerberg L, Hallström BM, Oksvold P, Kampf C, Djureinovic D, Odeberg J, Habuka M, Tahmasebpoor S, Danielsson A, Edlund K, Asplund A, Sjöstedt E, Lundberg E, Szigyarto CA, Skogs M, Takanen JO, Berling H, Tegel H, Mulder J, Nilsson P, Schwenk JM, Lindskog C, Danielsson F, Mardinoglu A, Sivertsson A, von Feilitzen K, Forsberg M, Zwahlen M, Olsson I, Navani S, Huss M, Nielsen J, Ponten F, Uhlén M. Analysis of the human tissue-specific expression by genome-wide integration of transcriptomics and antibody-based proteomics. *Mol Cell Proteomics.* 2014;13:397–406. <https://doi.org/10.1074/mcp.M113.035600>.
35. Usai M, Veyrenre S, Darracq M, Regnault C, Sroda S, Fini JB, Canlet C, Tremblay-Franco M, Ravetton M, Reynaud S. Transgenerational metabolic disorders and reproduction defects induced by benzo[a]pyrene in *Xenopus tropicalis*. *Environ Pollut.* 2021;269:116109. <https://doi.org/10.1016/j.envpol.2020.116109>.
36. Brodie ED Jr, Gibson LS. Defensive behavior and skin glands of the North-western salamander, *Ambystoma gracile*. *Herpetologica.* 1969;25:187–94.
37. Brizzi R, Delfino G, Jantra S, Alvarez BB, Sever DM. The amphibian cutaneous glands: some aspects of their structure and adaptive role. In: Lymberakis P, Valakos E, Pafilis P, Mylonas M, editors. *Herpetologia Candiana*. Crete: National Museum of Crete; 2001.
38. Almeida PG, Felsenburgh FA, Azevedo RA, Brito-Gitirana L. Morphological re-evaluation of the parotoid glands of *Bufo ictericus* (Amphibia, Anura, Bufonidae). *Contrib Zool.* 2007;76:145–52. <https://doi.org/10.1163/18759866-07603001>.
39. Blennenhassett RA, Bell-Anderson K, Shine R, Brown GP. The cost of chemical defence: the impact of toxin depletion on growth and behaviour of cane toads (*Rhinella marina*). *Proc R Soc B.* 2019;286:20190867. <https://doi.org/10.1098/rspb.2019.0867>.
40. Hattori T, Takei N, Mizuno Y, Kato K, Kohsaka S. Neurotrophic and neuroprotective effects of neuron-specific enolase on cultured neurons from embryonic rat brain. *Neurosci Res.* 1995;21:191–8. [https://doi.org/10.1016/0168-0102\(94\)00849-B](https://doi.org/10.1016/0168-0102(94)00849-B).
41. Vizin T, Kos J. Gamma-enolase: a well-known tumour marker, with a less-known role in cancer. *Radiol Oncol.* 2015;49:217–26. <https://doi.org/10.1515/raon-2015-0035>.
42. Bärtsch P, Haerberli A, Straub PW. Blood coagulation after long distance running: Antithrombin III prevents fibrin formation. *Thromb Haemost.* 1990;63:430–4. <https://doi.org/10.1055/s-0038-1645060>.
43. Butenas S, Mann KG. Blood coagulation. *Biochem Mosc.* 2002;67:3–12. <https://doi.org/10.1023/A:1013985911759>.
44. Constat DB, Tobler AR, Rensing-Ehl A, Kemler I, Hersh LB, Fontana A. Puromycin-sensitive aminopeptidase. Sequence analysis, expression, and functional characterization. *J Biol Chem.* 1995;270:26931–9. <https://doi.org/10.1074/jbc.270.45.26931>.
45. Tanahashi N, Kawahara H, Murakami Y, Tanaka K. The proteasome-dependent proteolytic system. *Mol Biol Rep.* 1999;26:3–9. <https://doi.org/10.1023/A:1006909522731>.
46. Shringarpure R, Grune T, Davies KJA. Protein oxidation and 20S proteasome-dependent proteolysis in mammalian cells. *CMLS Cell Mol Life Sci.* 2001;58:1442–50. <https://doi.org/10.1007/PL00000787>.
47. Jansen RS, Addie R, Merkx R, Fish A, Mahakena S, Bleijerveld OB, Altelaar M, IJlst L, Wanders RJ, Borst P, van de Wetering K. N-lactoyl-amino acids are ubiquitous metabolites that originate from CNDP2-mediated reverse proteolysis of lactate and amino acids. *PNAS.* 2015;112:6601–6. <https://doi.org/10.1073/pnas.1424638112>.
48. Winder SJ, Walsh MP. Calponin: thin filament-linked regulation of smooth muscle contraction. *Cell Signal.* 1993;5:677–86.
49. Allen BG, Walsh MP. The biochemical basis of the regulation of smooth-muscle contraction. *Trends Biochem Sci.* 1994;19:362–8.
50. Matyushenko AM, Shchepkin DV, Kopylova GV, Bershtsky SY, Levitsky DI. Unique functional properties of slow skeletal muscle tropomyosin. *Biochimie.* 2020;174:1–8. <https://doi.org/10.1016/j.biochi.2020.03.013>.
51. Cheung WY. Calmodulin. *Sci Am.* 1982;246:62–72.
52. Wright SC, Schellenberger U, Ji L, Wang H, Lerrick JW. Calmodulin-dependent protein kinase II mediates signal transduction in apoptosis. *FASEB J.* 1997;11:825–921. <https://doi.org/10.1096/fasebj.11.11.9285482>.
53. Hu J, Shi D, Ding M, Huang T, Gu R, Xiao J, Xian CJ, Dong J, Wang L, Liao H. Calmodulin-dependent signalling pathways are activated and mediate the acute inflammatory response of injured skeletal muscle. *J Physiol.* 2019;597:5161–77. <https://doi.org/10.1113/JP278478>.
54. Danzer KM, Ruf WP, Putcha P, Joyner D, Hashimoto T, Glabe C, Hyman BT, McLean PJ. Heat-shock protein 70 modulates toxic extracellular α -synuclein oligomers and rescues trans-synaptic toxicity. *FASEB J.* 2011;25:326–36. <https://doi.org/10.1096/fj.10-164624>.
55. Levine SD, Kachadorian WA, Levin DN, Schlondorff D. Effects of trifluoperazine on function and structure of toad urinary bladder. Role of calmodulin vasopressin-stimulation of water permeability. *J Clin Invest.* 1981;67:662–72. <https://doi.org/10.1172/JCI110081>.
56. Crespo CA, Medina MF, Ramos I, Fernández SN. Homeostasis and secretion of calcium in the oviductal mucosa of toad *Rhinella arenarum*. *J Exp Zool A.* 2014;321:432–41.
57. Torda C. Illumination dependent hyperpolarization of the photoreceptor outer segment membrane (role of calcium, cyclic GMP and calmodulin). *Int J Neurosci.* 1981;14:153–61. <https://doi.org/10.3109/00207458108985828>.
58. Smith DG, Rogers DC, Chamley-Campbell J, Campbell GR. The mechanism of blood flow redistribution within the carotid labyrinth of the toad, *Bufo marinus*. *J Exp Zool.* 1981;216:387–94.
59. Bulbul U, Kutrup B. Interspecific differences in molecular weights of skeletal myosin, actin, troponin C and tropomyosin in the frogs *Hyla japonica* and *Xenopus tropicalis*. *Biol Bratisl.* 2007;62:781–5. <https://doi.org/10.2478/s11756-007-0136-y>.
60. Cruetz CE. The annexins and exocytosis. *Science.* 1992;258:924–31. <https://doi.org/10.1126/science.1439804>.
61. Futter CE, White IJ. Annexins and endocytosis. *Traffic.* 2007;8:951–8. <https://doi.org/10.1111/j.1600-0854.2007.00590.x>.
62. Kragelund BB, Knudsen J, Poulsen FM. Acyl-coenzyme A binding protein (ACBP). *Biochim Biophys Acta Bioenerg.* 1999;1441:150–61.
63. Zhang Y, Yu G, Wang Y, Zhang J, Wei S, Lee W, Zhang Y. A novel annexin A2 protein with platelet aggregation-inhibiting activity from amphibian *Bombina maxima* skin. *Toxicol.* 2010;56:458–65. <https://doi.org/10.1016/j.toxicon.2010.04.015>.
64. Xiao XH, Miao HM, Xu YG, Zhang JY, Chai LH, Xu JJ. Analysis of skin and secretions of Dybowsky's frogs (*Rana dybowskii*) exposed to *Staphylococcus aureus* or *Escherichia coli* identifies immune response proteins. *Vet J.* 2014;200:127–32. <https://doi.org/10.1016/j.tvjl.2014.01.011>.
65. Geng X, Wei H, Shang H, Zhou M, Chen B, Zhang F, Zang X, Li P, Sun J, Che J, Zhang Y, Xu C. Proteomic analysis of the skin of Chinese giant salamander (*Andrias davidianus*). *J Proteomics.* 2015;119:196–208. <https://doi.org/10.1016/j.jprot.2015.02.008>.
66. Barra D, Simmaco M. Amphibian skin: a promising resource for antimicrobial peptides. *Trends Biotechnol.* 1995;13:205–9. [https://doi.org/10.1016/S0167-7799\(00\)88947-7](https://doi.org/10.1016/S0167-7799(00)88947-7).
67. Rinaldi AC. Antimicrobial peptides from amphibian skin: an expanding scenario: commentary. *Curr Opin Chem Biol.* 2002;6:799–804. [https://doi.org/10.1016/S1367-5931\(02\)00401-5](https://doi.org/10.1016/S1367-5931(02)00401-5).

68. Pukala TL, Bowie JH, Maselli VM, Musgrave IF, Tyler MJ. Host-defence peptides from the glandular secretions of amphibians: structure and activity. *Nat Prod Rep.* 2006;23:368–93. <https://doi.org/10.1039/B512118N>.
69. Pisochni AM, Pop A. The role of antioxidants in the chemistry of oxidative stress: a review. *Eur J Med Chem.* 2015;97:55–74. <https://doi.org/10.1016/j.ejmech.2015.04.040>.
70. Barja de Quiroga G, Gil P, López-Torres M. Physiological significance of catalase and glutathione peroxidases, and *in vivo* peroxidation, in selected tissues of the toad *Discoglossus pictus* (Amphibia) during acclimation to normobaric hyperoxia. *J Comp Physiol B.* 1988;158:583–90.
71. Stuart SN, Chanson JS, Cox NA, Young BE, Rodrigues ASL, Fischman DL, Waller RW. Status and trends of amphibian declines and extinctions worldwide. *Science.* 2004;306(5702):1783–6. <https://doi.org/10.1126/science.1103538>.
72. Blaustein AR, Belden LK, Hatch AC, Kats LB, Hoffman PD, Hays JB, Marco A, Chivers DP, Kiesecker JM. Ultraviolet radiation and amphibians. In: Cockell CS, Blaustein AR, editors. *Ecosystems, evolution, and ultraviolet radiation.* New York: Springer; 2001. p. 63–79. https://doi.org/10.1007/978-1-4757-3486-7_3.
73. Licht LE, Grant KP. The effects of ultraviolet radiation on the biology of amphibians. *Am Zool.* 1997;37:137–45. <https://doi.org/10.1093/icb/37.2.137>.
74. Schuch AP, Lipinski VM, Santos MB, Santos CP, Jardim SS, Cechin SZ, Loreto ELS. Molecular and sensory mechanisms to mitigate sunlight-induced DNA damage in treefrog tadpoles. *J Exp Biol.* 2015;218:3059–67. <https://doi.org/10.1242/jeb.126672>.
75. Morimoto R, Santoro M. Stress-inducible responses and heat shock proteins: new pharmacologic targets for cytoprotection. *Nat Biotechnol.* 1998;16:833–8. <https://doi.org/10.1038/nbt0998-833>.
76. Wang RE. Targeting heat shock proteins 70/90 and proteasome for cancer therapy. *Curr Med Chem.* 2011;18:4250–64. <https://doi.org/10.2174/092986711797189574>.
77. Storey JM, Storey KB. In defense of proteins: chaperones respond to freezing, anoxia, or dehydration stress in tissues of freeze tolerant wood frogs. *J Exp Zool A.* 2019;331:392–402. <https://doi.org/10.1002/jez.2306>.
78. Wu CW, Tessier SN, Storey KB. Dehydration stress alters the mitogen-activated-protein kinase signaling and chaperone stress response in *Xenopus laevis*. *Comp Biochem Physiol B.* 2020;246–247:110461. <https://doi.org/10.1016/j.cbpb.2020.110461>.

Publisher's Note

Springer Nature remains neutral with regard to jurisdictional claims in published maps and institutional affiliations.

Ready to submit your research? Choose BMC and benefit from:

- fast, convenient online submission
- thorough peer review by experienced researchers in your field
- rapid publication on acceptance
- support for research data, including large and complex data types
- gold Open Access which fosters wider collaboration and increased citations
- maximum visibility for your research: over 100M website views per year

At BMC, research is always in progress.

Learn more biomedcentral.com/submissions

